RSC Advances

RSC Publishing

PAPER

View Article Online
View Journal | View Issue

Cite this: *RSC Advances*, 2013, **3**, 18849

Moisture-resistant porous polymer from concentrated emulsion as low-cost and high-capacity sorbent for CO_2 capture

Zuolong Liu,[a] Zhongjie Du,[a] Wei Zou,[a] Jianguo Mi,[b] Hangquan Li,[a] Yihan Wang[a] and Chen Zhang*[a]

Received 13th July 2013,
Accepted 5th August 2013

DOI: 10.1039/c3ra43597k

www.rsc.org/advances

A moisture-resistant CO_2 adsorbent was designed and prepared. The adsorbent used porous polystyrene as a skeleton, surface modified with amine groups. The structure and morphology of the adsorbent were characterized using infrared spectroscopy, scanning electron microscopy, and energy-dispersive spectrometry. Due to the huge specific surface area covered by a large number of amine groups, such porous material could be applied for capturing carbon dioxide under atmospheric pressure. Under a pressure of 100 Kpa, 3.46 mmol g^{-1} of CO_2 adsorption uptake was observed. The porous adsorbent also exhibited a high CO_2 adsorption rate, excellent moisture resistance, good selectivity for CO_2–N_2 separation, and easy CO_2 regeneration.

1. Introduction

CO_2 capture, utilization, and storage (CCUS) technology on flue gases constitute a useful measure to reduce global warming.[1,2] Whatever the secondary use, CO_2 capture was considered a key step.[3,4] For this reason, plenty of effort has been expended on developing technology for efficient CO_2 capture. The current industrial technology for CO_2 capture from flue gas is based on liquid amines, especially monoethanolamine and diethanolamine (MEA and DEA).[5–7] However, problems such as high regeneration energy, large equipment size, solvent degradation, and equipment corrosion made the process impractical for further applications.[8,9] In order to overcome the limitation of liquid amine-based processes, research has focused on solid adsorption materials because of their low energy consumption and low equipment cost. A large number of solid CO_2 adsorbents were developed by anchoring amine-groups on the surface of porous matrices including mesoporous poly(ionic liquid),[10] microporous organic polymers (MOPs),[11] nanoparticulate organic hybrid materials,[12] zeolites,[13,14] activated carbons,[15,16] periodic mesoporous silicas[17] as well as metal organic frameworks (MOFs).[18,19] The amine functionalization of the adsorbent matrix was usually carried out by two approaches: surface grafting and impregnation. Although the adsorbents based on the latter could carry more amine groups than the former, however, the impregnated amine groups would hinder the diffusion of CO_2 molecules in the porous matrix and thus reduce the efficacy in both adsorption and regeneration.[20] In comparison, the approach of grafting was preferred and significant effort was directed towards fixing amine groups onto porous material surfaces.[21]

Organic materials, especially porous polymers, may provide more active sites for fixing amine groups and have advantages like facile processing, easy surface modification, and low cost.[22,23] Porous polymer materials have been widely applied in the biomedical and pharmaceutical fields,[24,25] chromatographic media,[26] catalysis of chemical and biochemical reactions,[27] and electronic devices.[28] Among various preparative approaches, concentrated emulsion (dispersed phase volume >74%) templating[29] constituted a flexible and easily controlled method in the fabrication of interconnected porous materials. In recent decades, extensive studies have been conducted to improve the adsorption capacity of sorbents through increasing the specific surface area of porous organic polymers[30,31] for sequestration of CO_2. However, most of these materials lacked good resistance to water, and moisture was one of the key components in flue gas that could compete with CO_2 for adsorption sites and thus decreased the adsorption capacity.[32] In general, carbon dioxide capture from flue gas needed a drying process before the adsorption, which would increase the energy consumption. Therefore, the development of moisture-resistant adsorbent for carbon dioxide capture would be crucial for an effective and energy-saving process.

In this work, a polystyrene skeleton with an interconnected porous structure was first prepared through a concentrated emulsion polymerization approach, and the surface of porous

[a]*Key Laboratory of Carbon Fiber and Functional Polymers, Ministry of Education, Beijing University of Chemical Technology, Beijing 100029, P. R. China. E-mail: zhangch@mail.buct.edu.cn; Fax: +86-10-64428804; Tel: +86-10-64428804*
[b]*State Key Laboratory of inorganic and organic materials, Beijing University of Chemical Technology, Beijing 100029, P. R. China*

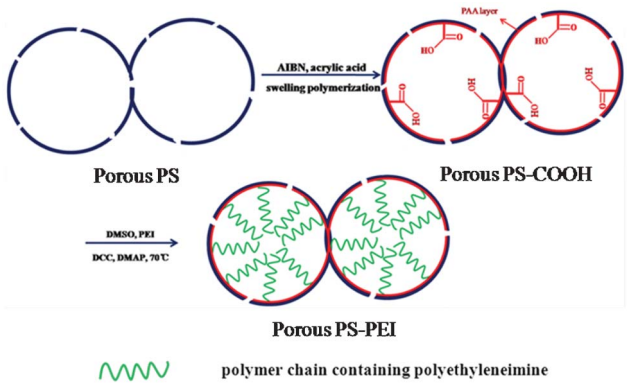

Scheme 1 The preparation process for porous PS-NH_2.

skeleton was subsequently modified with polyacrylic acid and then with polyethylene imine (Scheme 1). Polyacrylic acid acted as a hydrophilic layer which could absorb water molecules of the flue gas. As a result, the CO_2 absorption capacity of sorbent could increase in the presence of a certain amount of water. In addition, acrylic acid macromolecules could also provide active sites to react with more polyethylene imine. Finally, an effective and energy-saving CO_2 adsorbent was obtained. It was showed that in addition to its outstanding CO_2 capture capacity, the porous adsorbent exhibited an easy CO_2 regeneration behaviour at relatively low temperatures (110 °C) and an excellent stability over 10 adsorption–desorption cycles. Such novel adsorbent was significant for industrial applications.

2. Experimental

2.1 Materials

Styrene (St), divinylbenzene (DVB, containing 20% ethylstyrene), and azobisisobutyronitrile (AIBN, AR) were supplied by Beijing Chemical Reagent Co., China. Acrylic acid (AA, CP) was provided by Tianjin Chemical Research Institute. Polyethylene imine (PEI, MW = 10 000), sorbitan monooleate (SMO, Span80), potassium persulfate ($K_2S_2O_8$), potassium sulfate (K_2SO_4), dicyclohexylcarbodiimide (DCC), 4-dimethylaminopyridine (DMAP), dimethyl sulfoxide (DMSO), methanol, and toluene were purchased from Vas Chemical Co., China. Styrene was distilled and AIBN was recrystallized from methanol before use.

2.2 Preparation of porous polystyrene

The synthesis procedure was described in one of our previous works[33] and was modified to obtain a high specific surface area. Briefly, an aqueous phase (water 90 ml, $K_2S_2O_8$ 0.15 g, and K_2SO_4 0.376 g) was added slowly to an organic phase consisting of St 5 ml, DVB 5 ml, SMO 3 ml, and toluene (0 ml, 5 ml, 10 ml, or 15 ml). With stirring, a concentrated emulsion was obtained with the organic phase being the continuous one. Subsequently, the concentrated emulsion was heated to 65 °C and kept for 24 h, and a porous polystyrene was obtained. The product was soaked in water for 24 h, in methanol for 24 h, and then dried in a convection oven at 60 °C until a constant weight was achieved. The obtained porous polystyrene was cut into small blocks of about 1 cm^3 and further extracted with refluxing ethanol in a Soxhlet apparatus (typically 2–3 days) and finally dried in a vacuum oven at room temperature and was denoted as porous PS in what follows.

2.3 Surface modification with carboxyl groups

5 g of porous PS blocks was soaked in a 100 g toluene solution containing 10 g AIBN for 3 h, and AIBN was introduced into the surface of porous PS by a slight swelling of the porous PS. Then the blocks were dried to remove toluene and the initiator AIBN was fixed. Subsequently, the blocks were soaked in 100 ml water containing 5 wt% acrylic acid, and a vacuum was applied for 24 h to help the solution permeate into the blocks. The blocks in acrylic acid aqueous solution were transferred into a glass vessel and heated at 60 °C for 24 h. After the polymerization of acrylic acid initiated by the AIBN fixed on the surface of the porous PS, a thin layer of poly(acrylic acid) (PAA) was coated on the surface and was denoted as porous PS-COOH in what follows. The unreacted acrylic acid was removed with water and the porous PS-COOH was dried in a vacuum oven at 60 °C until a constant weight was achieved.

2.4 Surface modification with amine groups

5 g of porous PS-COOH was soaked in a mixture of 100 ml dry DMSO, 10 g of PEI, 1 g of DCC, and 0.1 g of DMAP under a vacuum for 24 h. Then the mixture was heated to 70 °C and kept for 24 h. A small fraction of amine groups on the PEI were reacted with carboxyl groups on the PAA to graft PEI onto the PAA layer, while most amino groups remained on the surface of the porous polystyrene. After the reaction, the blocks were cooled to room temperature, washed with CH_2Cl_2 and water, and dried under vacuum. A pale yellow product was obtained which would be used as the solid adsorbent and was denoted as porous PS-PEI in what follows.

2.5 Characterization

The porous morphology was viewed from a cryogenic fractured surface using high resolution scanning electron microscopy (SEM, Japan, Hitachi LtdS-4700). Elemental analysis was performed on an Hitachi LtdS-4700 field emission scanning electron microscope (FE-SEM) equipped with an energy-dispersive spectrometer (EDS) produced by EDAX Inc. The chemical structures were detected using a Fourier transfer infrared spectrometer (FT-IR, Thermo Nicolet-Nexus670). The specific surface area was determined using the Brunauer–Emmett–Teller (BET) method based on N_2 adsorption data in the relative pressure range of 0.06–0.22. The total pore volume was estimated from the amount adsorbed at a relative pressure of P/P_0 = 0.95. The porosity was observed by using a Helium porosimeter (Core Test Inc., model PHI-220). The porous material was dried at 100 °C in a vacuum oven for 3 h and then cooled to room temperature. The porosity was determined by dividing the pore volume of sample by its bulk volume.

Adsorption isotherms of CO_2 and N_2 were measured using a Micromeritics ASAP 2020. The adsorption run was carried out

using highly pure CO_2 (99.99%) at a pressure between 0.01 and 100 kPa depending on the temperature. In order to remove any impurities, the adsorbent was firstly outgassed in vacuum at 120 °C for 12 h. Desorption was carried out at a temperature of 110 °C under pure N_2 for 30 min. The adsorbent was regenerated using vacuum and temperature swing adsorption (VTSA) regeneration.[34,35] The stability was evaluated in adsorption–desorption cycles. The sample was first pre-treated in flowing dry N_2 at 100 °C and then cooled to 40 °C before switching to pure CO_2 for 30 min. The adsorption of CO_2 from CO_2–N_2 binary mixture was performed using a self-restraint experimental apparatus at Tsinghua University, China. The test process and calculated separation factors were previously described in detail.[36] A fixed-bed flow sorber (a stainless steel tube with an inner diameter of 16 mm and a length of 200 mm) operated at 1 bar and 40 °C, which was controlled by a pressure controller and a thermostatic water bath. The sorbent bed was first heated to 110 °C in N_2 at a flow rate of 100 ml min^{-1} and held for 30 min. A breakthrough experiment was carried out by switching abruptly from N_2 to a 14% mixture of CO_2 in N_2 and at a flow rate of 7 ml min^{-1}. The treated gas out of the sorbent was monitored online using an Agilent 6890 gas chromatograph with a TCD detector. The pH value of the water absorbed by the adsorbent was measured using a Testo206 PH_2 (Germany).

3. Results and discussion

3.1 Concentrated emulsion-templated porous polystyrene

SEM images of the porous PS prepared through the concentrated emulsion polymerization with various volume fractions of the dispersed phase (Φ) are presented in Fig. 1. They all showed spherical cells connected with small intercellular pores. One may notice that when Φ was between 0.8 and 0.9, the pore size decreased with the increasing Φ value, accompanied by a decreasing thickness of the continuous wall. However, when Φ was 0.95, the pore size became inhomogeneous, which was a result of instability of the concentrated emulsion. To be an efficient CO_2 adsorbent, it should have a higher specific surface area to support a large amount of amine groups. In general, a smaller pore size resulted in a larger specific surface area. As shown in Table 1, when Φ increased from 0.80 to 0.95, the specific surface area, volume of pores, and porosity of the porous PS increased from 16 to 42 $m^2\ g^{-1}$, 0.06 to 0.18 $cm^3\ g^{-1}$, and 31.6 to 74.8%, respectively. Because of the instability of the concentrated emulsion with Φ = 0.95, the following discussion is exclusively based on porous PS prepared from concentrated emulsion with Φ = 0.90.

Table 1 Porosities of porous PS samples based on the different volume fractions of dispersed phase (Φ)

Φ	Specific surface area ($m^2\ g^{-1}$)	Volume of pores ($cm^3\ g^{-1}$)	Porosity (%)
0.80	16	0.06	34.6
0.85	24	0.09	53.2
0.90	35	0.15	71.5
0.95	42	0.18	74.8

In order to further increase the specific surface area of the porous matrix, a non-reactive solvent (porogen) was introduced into the continuous phase. In this work, toluene was chosen as a porogen for the porous PS. The SEM micrographs of the porous PS containing various contents of porogen are presented in Fig. 2. One may noticed that the porogen resulted in small spherical holes on the wall of large pores, which greatly enlarged the specific surface area of the material. As listed in Table 2, when the weight ratio of porogen to monomer was 1/1, a specific surface area of 247 $m^2\ g^{-1}$ was obtained. However, when too much porogen was introduced, the concentrated emulsion became unstable. Therefore, this work was focused on the system with a weight ratio of porogen over monomer equal to 1/1.

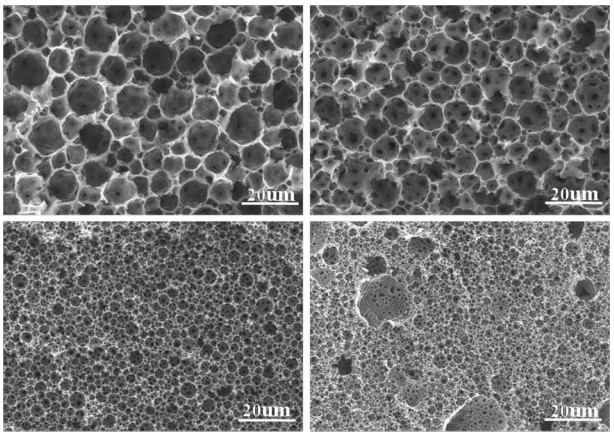

Fig. 1 SEM images of porous PS obtained from concentrated emulsion polymerization. The volume fraction of dispersed phase: (a) 80%; (b) 85%; (c) 90%; (d) 95%.

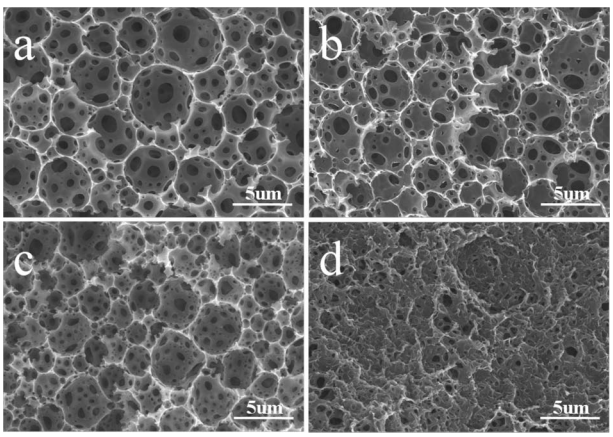

Fig. 2 SEM images of porous PS prepared with porogen toluene. The weight ratio of toluene to monomer: (a) 0/1; (b) 0.5/1; (c)/1/1; (d) 1.5/1.

Table 2 Porosities of porous PS samples based on different porogen contents

Weight ratio of porogen/monomer	Specific surface area ($m^2\ g^{-1}$)	Volume of pores ($cm^3\ g^{-1}$)
0/1	35	0.15
0.5/1	84	0.19
1/1	247	0.36
1.5/1	—	—

3.2 Characterization of porous PS-PEI

The FT-IR spectra of the porous monoliths are displayed in Fig. 3. In the spectrum of porous PS (Fig. 3a), there were characteristic peaks corresponding to benzene groups at 3025, 3059, 3081 cm^{-1} and to aliphatic C–H at 2853, 2924 cm^{-1}. After carboxylic groups were introduced, broad hydroxyl bands at 3450, 2570, and 1715 cm^{-1} were shown (Fig. 3b). In the spectrum of porous PS-PEI (Fig. 3c), the adsorption peaks at 3400, 3330 cm^{-1} for NH_2 and at 1627 cm^{-1} for amide groups were observed, which indicated the coating of PEI. At the same time, the above mentioned bands for carboxyl groups almost disappeared. It was deduced that amine-functionalization of the porous material was complete.

SEM micrographs of the porous monoliths in different preparation stages are presented in Fig. 4. For comparison of Fig. 4a with Fig. 4b, it found that the surface modification with poly(acrylic acid) (PAA) caused no obvious change in the porosity. This indicated that the quantity of PAA fixed on the surface of porous PS was very small. Since the polymerization of acrylic acid took place in the micro-pores, the diffusion of monomers was rather limited. However, after the surface was coated with PEI, most of the small holes were blocked and the walls of the pores were thickened, as shown in Fig. 4c. Because the molecular weight of PEI was high (10 000), a very small extent of coating may result in a large coverage on the surface. PEI molecules carried a large quantity of amine groups, which would play an important role in the CO_2 adsorption.

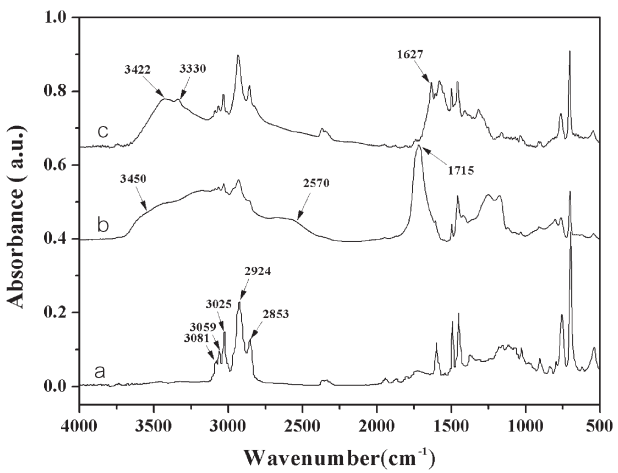

Fig. 3 FT-IR spectra of porous PS (a), porous PS-COOH (b) and porous PS-PEI (c).

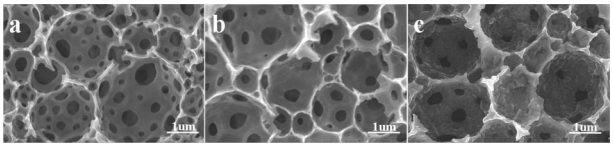

Fig. 4 SEM images of various porous samples: (a) porous PS; (b) porous PS-COOH; (c) porous PS-PEI.

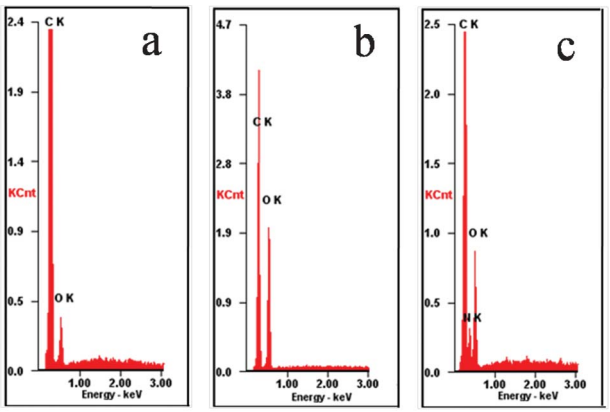

Fig. 5 EDS spectra of various porous samples: (a) porous PS; (b) porous PS-COOH; (c) porous PS-PEI.

The EDS results of various porous samples are presented in Fig. 5 and Table 3. It was clear that the oxygen and nitrogen atoms were introduced by PAA and PEI, respectively. Furthermore, a correlation between the CO_2 adsorption capacity and the N content of the amine-functionalized adsorbent was obvious.[37] The higher nitrogen content would lead to higher CO_2 adsorption capacity.

The effect of the contents of initiator (AIBN) and monomer (acrylic acid) on the quantity of coated PEI is presented in Tables 4 and 5. The effect of initiator is shown in Table 4, in which the concentration of acrylic acid in water was kept at 10 wt%. The coating content was calculated by the weight ratio of the coating layer to the porous monolith before modification. The maximum PEI coating was obtained when the initiator content was 10 wt%. The produced PAA molecular chains covering the surface of porous PS might block acrylic acid monomer from the initiator, and that was the reason for the lower content of PAA with higher initiator content. Moreover, because of the steric effects, if the surface coating on the porous PS was too high, the degree of reaction between PAA and PEI might decrease resulting in a low PEI content. Table 5

Table 3 Elemental composition of various porous samples

Samples	C (atom%)	O (atom%)	N (atom%)
Porous PS	94.6	5.4	
Porous PS-COOH	68.73	31.27	
Porous PS-PEI	68.13	15.75	16.12

Table 4 Effect of the concentration of initiator on the coating weight content of porous samples

Initiator concentration (%)	PAA coating content (%)	PEI coating content (%)
5	8.9	19.3
10	21.3	46.4
15	47.9	44.2
20	32.6	31.1

Table 5 Effect of the concentration of acrylic acid on the coating weight content of porous samples

Monomer concentration (%)	PAA coating content (%)	PEI coating content (%)
5	5.1	7.2
10	21.3	46.4
15	53.9	45.2
20	68.8	34.6

displays the effect of monomer concentration (acrylic acid in water solution) when the content of initiator was kept at 10 wt%. It was found that 10 wt% constituted the optimal monomer concentration for maximum coating of PEI. The reason was similar to the effect of the initiator content. The following discussion is based on the porous PS-PEI prepared using 10 wt% concentration of initiator (AIBN) in toluene and then 10 wt% concentration of acrylic acid in aqueous solution.

3.3 CO_2 adsorption of porous PS-PEI

Fig. 6 shows a plot of CO_2 adsorption efficiency for porous PS, porous PS-COOH, and porous PS-PEI. At a pressure of 100 kPa, the adsorption capacity of PS or PS-COOH was only about 0.13 mmol g^{-1}. After coating with PEI, the CO_2 adsorption capacity of porous PS-PEI was increased to 3.46 mmol g^{-1}, which was greater than the reported value of 2.5 mmol g^{-1} for SBA-15.[38]

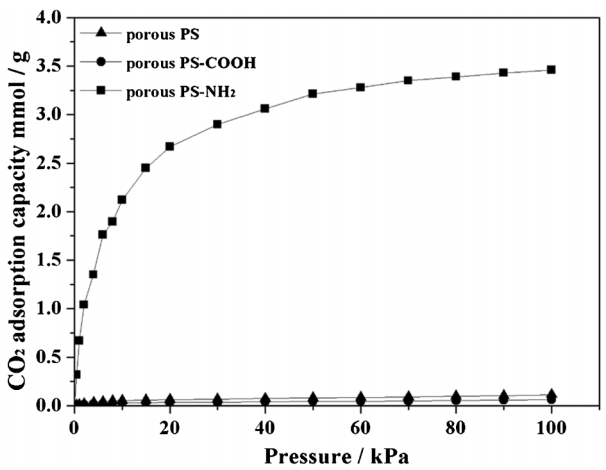

Fig. 6 A plot of CO_2 (CO_2 concentration: 99.99%) adsorption capacity for porous PS, porous PS-COOH, and porous PS-PEI at 40 °C.

Table 6 Characterisation of porous samples

Sample	N content (wt%)[a]	Surface area (m^2 g^{-1})	Volume of pores (cm^3 g^{-1})
Porous PS	—	247	0.36
Porous PS-COOH	—	132	0.15
Porous PS-PEI	10.94	34	0.06

Table 6 showed that the surface area and volume of pores of the porous PS were reduced after carboxylization and subsequent amine-coating. However, it was the amine groups introduced onto the surface that provided the sites to accommodate CO_2, and the material could be used as an adsorbent for CO_2 capture.

3.4 CO_2/N_2 selectivity adsorption and sorbent regeneration

For practical applications, in addition to a high CO_2 adsorption capacity, fast adsorption kinetics, a high selectivity towards CO_2 and reversible adsorption properties were required for a porous adsorbent. Fig. 7 shows the adsorption kinetics of CO_2 and N_2 on porous PS-PEI at 40 °C. It can be seen that the capture of CO_2 took place at a high adsorption rate, more than 95% of CO_2 being adsorbed in ~15 min. In contrast, N_2 adsorption occurred at a very low rate.

In addition to the equilibrium uptake measurements, dynamic "breakthrough" separation experiments on porous PS-PEI were conducted to determine its CO_2 separation capacity, using a flow of 14% (v/v) CO_2 mixed with N_2, which approximately mimicked a flue gas (Fig. 8). F was effluent volumetric gas flow rate (cm^3 min^{-1}) and F_0 was total volumetric gas flow rate (cm^3 min^{-1}). The result indicated that porous PS-PEI could completely separate CO_2 from the N_2 stream, and the separation factor for CO_2 over N_2 was estimated to be 26.9. The selectivity of porous PS-PEI was higher than that of the widely used BPL carbon (separation factors: 11.1)[39] or ZIF-79 (separation factors: about 22).[40] The

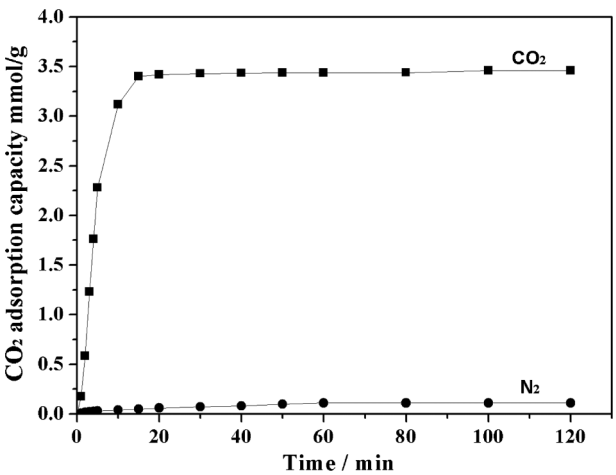

Fig. 7 Adsorption kinetics of CO_2 and N_2 at 40 °C for porous PS-PEI.

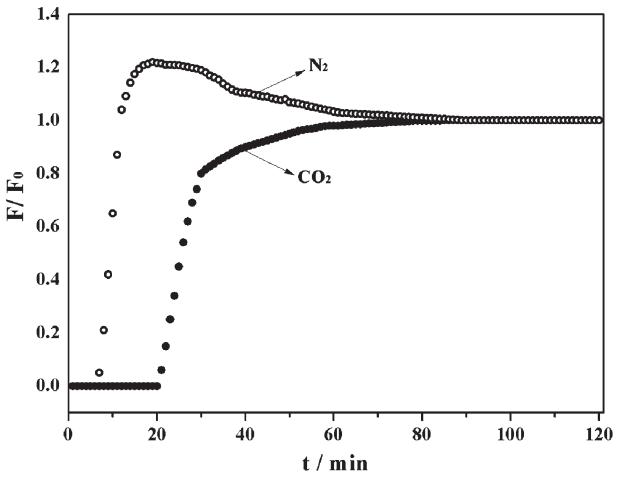

Fig. 8 Breakthrough curves, a 14% mixture of CO_2 in N_2 is fed into a bed of porous PS-PEI.

dynamic data provided clear evidence that porous PS-PEI was highly selective for adsorbing CO_2 over N_2.

Fig. 9 shows the CO_2 adsorption–desorption cycles obtained for porous PS-PEI at 40 °C (CO_2 concentration: 99.99%). In order to determine the stability of porous PS-PEI during the adsorption/desorption cycling, the sample was repeatedly heated to 110 °C under N_2 and then cooled to ambient under CO_2. As shown in Fig. 9, the reduction in CO_2 adsorption capacity was less than 2% after each run. This indicated both the porous structure and the attachment of the amine groups were stable during the heating–cooling cycles.

3.5 Effect of moisture

The effect of moisture content in the flue gas on the CO_2 adsorption of porous PS-PEI is shown in Table 7. One may notice that when moisture content was lower than 10%, the CO_2 adsorption capacity increased with increasing moisture content;

Table 7 Effect of moisture concentrations on CO_2 adsorption capacity of porous PS-PEI and PH of absorbed water

Water content of porous PS-PEI	0%	5%	10%	15%
Adsorption uptake (mmol g^{-1})	3.46	3.65	3.81	3.77
PH of absorbed water	7.00	8.89	8.93	8.92

in other words, the presence of moisture promoted the adsorption of CO_2. In contrast, for conventional adsorbents like zeolites, the capacity of CO_2 adsorption would be dramatically reduced by moisture. This comparison implied that the synthesized amino-functionalized porous PS adsorbent had potential applicability in environments for CO_2 adsorption where water was inevitable. This promoting effect of water could be explained on the basis of the reactions between CO_2 and amine groups. Such reaction could give carbamic acids and urea. During the reaction, water could be deprotonated by amine (giving an ammonium cation) and the resulting hydroxide anion could react with CO_2 to give bicarbonate.[32,41] As a result, the pH of the absorbed water would increase (Table 7). For a water content of 5%, the FT-IR spectra of PS-PEI before and after CO_2 capture are shown in Fig. 10. The new absorption bands at 1650, 1540, and 1407 cm^{-1} assigned to N–H deformation in RNH_3^+, C=O stretch, and NCOO skeletal vibration, respectively, appeared after the CO_2 adsorption, which could be a good indication of the formation of bicarbonate and carbamate. The band at 2460 cm^{-1} after CO_2 capture was also the result of chemically absorbed CO_2 species.[42]

Under dry conditions, where H_2O and OH^- were absent, the maximum amine efficiency of an amine adsorbent was 0.5 mol CO_2 per 1 mol N. Amine efficiency is defined here as the number of moles of CO_2 captured per unit mass of amine divided by the moles of N per unit mass of amine. Under humid conditions, where H_2O could act as a base, the maximum amine efficiency was 1 mol CO_2 per 1 mol N.[32] Therefore, moisture

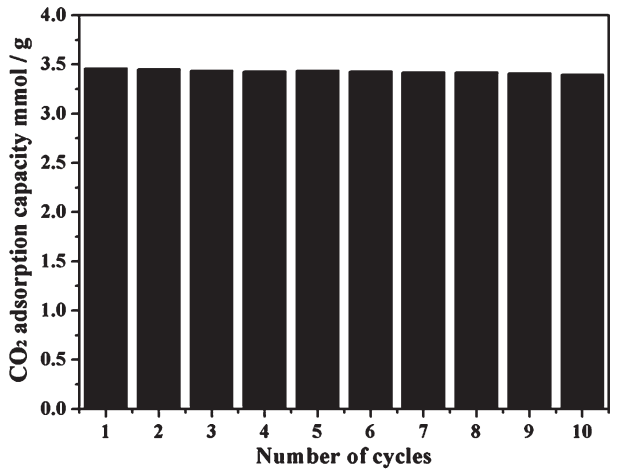

Fig. 9 CO_2 Adsorption–desorption cycles obtained for porous PS-PEI at 40 °C (CO_2 concentration: 99.99%).

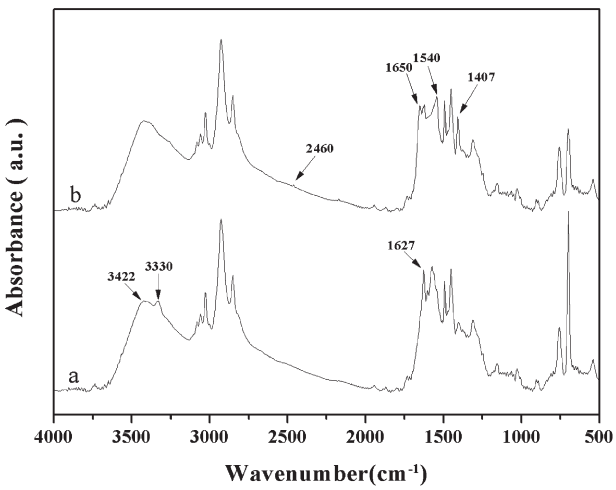

Fig. 10 FT-IR spectra of porous PS-PEI before (a) and after (b) CO_2–H_2O capture.

could enhance the adsorption of CO_2 on the amino-functionalized porous polystyrene. However, at too high moisture contents, the adsorption capacity was decreased. This behaviour may be associated with the competitive adsorption between CO_2 and H_2O at the same adsorption sites, which is in agreement with the result in the literature.[43]

4. Conclusions

An approach to a highly efficient organic CO_2 adsorbent material was proposed. A porous polystyrene based on concentrated emulsion templating was surface swollen with acrylic acid and its initiator, and the system was allowed to carry out a polymerization, resulting in a thin layer of poly(acrylic acid) coated on the bulk. The material obtained was subsequently grafted with polyethylene imine. Such specially designed CO_2 adsorbent displayed an exceptional capturing performance of up to 3.46 mmol g^{-1} under 100 kPa pressure and was extremely selective for adsorbing CO_2 over N_2. It could be readily and fully regenerated at relatively low temperature and exhibited excellent stability over repetitive adsorption–desorption cycles. In addition, the adsorbent was moisture tolerant, and the adsorption capacity could even be enhanced at moderate moisture contents. In this regard, the prepared porous PS-PEI offered a potential application with respect to the CO_2 adsorption industry.

Acknowledgements

This work is supported by the State Key Laboratory of Chemical Engineering, Tsinghua University, Beijing, China. (No. SKL-ChE-11A03).

References

1 B. C. Liu, C. Li, A. N. Sun and J. Zhang, *Adv. Mater. Res.*, 2012, **512–515**, 1282–1287.
2 F. S. Su, C. Y. Lu and H. Chen, *Langmuir*, 2011, **27**(13), 8090–8098.
3 S. Robert, *Science*, 2004, **13**, 305.
4 A. Harry, *Energy*, 1997, **22**(2–3), 217–221.
5 R. Bounaceur, N. Lape, D. Roizard, C. Vallieres and E. Favre, *Energy*, 2006, **31**, 2556.
6 B. R. Edward, S. A. Sami and C. S. Orville, *Ind. Eng. Chem. Res.*, 2000, **39**, 4346.
7 X. Zhang, C. F. Zhang, S. J. Qin and Z. S. Zheng, *Ind. Eng. Chem. Res.*, 2001, **40**, 3785.
8 A. Veawab, P. Tontiwachwuthikul and A. Chakma, *Ind. Eng. Chem. Res.*, 1999, **38**, 3917.
9 A. O. Babatunde and T. R. Gary, *AIChE J.*, 2007, **53**, 3144.
10 A. Wilke, J. Y. Yuan, M. Antonietti and J. Weber, *ACS Macro Lett.*, 2012, **1**, 1028–1031.
11 Q. Chen, M. Luo, P. Hammershoj, D. Zhou, Y. Han, B. W. Laursen, C. G. Yan and B. H. Han, *J. Am. Chem. Soc.*, 2012, **134**, 6084–6087.
12 C. Petit, Y. Park, K. A. Lin and A. A. Park, *J. Phys. Chem. C*, 2012, **116**, 516–525.
13 N. Konduru, P. Lindner and N. M. Assaf-Anid, *AIChE J.*, 2007, **53**, 3137.
14 R. Ghezini, M. Sassi and A. Bengueddach, *Microporous Mesoporous Mater.*, 2008, **113**, 370.
15 R. V. Siriwardane, M. S. Shen, E. P. Fisher and J. A. Poston, *Energy Fuels*, 2001, **15**, 279.
16 C. Pevida, T. C. Drage and C. E. Snape, *Carbon*, 2008, **46**, 1464.
17 Y. Belmabkhout, R. S. Guerrero and A. Sayari, *Chem. Eng. Sci.*, 2009, **64**, 3721.
18 S. R. Caskey, A. G. Wong-Foy and A. J. Matzger, *J. Am. Chem. Soc.*, 2008, **130**, 10870.
19 R. Babarao, J. W. Jiang and S. I. Sandler, *Energy Fuels*, 2010, **24**, 5273–5280.
20 W. J. Son, J. S. Choi and W. S. Ahn, *Microporous Mesoporous Mater.*, 2008, **142**, 564.
21 C. Knofel, C. Martin, V. Hornebecq and P. L. Llewellyn, *J. Phys. Chem. C*, 2009, **113**, 21726–21734.
22 A. Thomas, P. Kuhn, J. Weber, M. M. Titirici and M. Antonietti, *Macromol. Rapid Commun.*, 2009, **30**, 221–236.
23 H. Kim, Y. Kim, M. Yoon, S. Lim, S. M. Park, G. Seo and K. Kim, *J. Am. Chem. Soc.*, 2010, **132**, 12200–12202.
24 J. L. Drury and D. J. Mooney, *Biomaterials*, 2003, **24**, 4337–4351.
25 G. Akay, M. A. Birch and M. A. Bokhari, *Biomaterials*, 2004, **25**, 3991–4000.
26 D. R. Rolison, *Science*, 2003, **299**, 1698–1701.
27 H. Zou, X. Huang, M. Ye and Q. Luo, *J. Chromatogr., A*, 2002, **954**, 5–32.
28 C. G. Wu, M. I. Lu and H. J. Chuang, *Polymer*, 2005, **46**, 5929–5938.
29 N. R. Cameron and D. C. Sherrington, *Adv. Polym. Sci.*, 1996, **126**, 163–213.
30 R. Dawson, E. Stocked, J. R. Holst and A. I. Cooper, *Energy Environ. Sci.*, 2011, **4**, 4239–4245.
31 M. Kaliva, G. S. Armatas and M. Vamvakaki, *Langmuir*, 2012, **28**, 2690–2695.
32 S. Choi, J. H. Drese and C. W. Jones, *ChemSusChem*, 2009, **2**, 796–854.
33 X. Li, C. Zhang, Z. J. Du and H. Q. Li, *J. Colloid Interface Sci.*, 2008, **323**, 120–125.
34 M. G. Plaza, S. Garcia, F. Rubiera, J. J. Pis and C. Pevida, *Chem. Eng. J.*, 2010, **163**, 41–47.
35 G. D. Pirngruber, S. Cassiano-Gaspar, S. Louret, A. Chaumonnot and B. Delfort, *Energy Proc.*, 2009, **1**, 1335–1342.
36 G. P. Hao, W. C. Li, D. Qian, G. H. Wang, W. P. Zhang, T. Zhang, A. Q. Wang, F. Schuth, H. J. Bongard and A. H. Lu, *J. Am. Chem. Soc.*, 2011, **133**, 11378–11388.
37 W. Chaikittisilp, R. Khunsupat, T. T. Chen and C. W. Jones, *Ind. Eng. Chem. Res.*, 2011, **50**, 14203–14210.
38 S. Y. Hao, H. Chang, Q. Xiao, Y. J. Zhong and W. D. Zhu, *J. Phys. Chem. C*, 2011, **115**, 12873–12882.
39 R. Banerjee, H. Furukawa, D. Britt, C. Knobler, M. O'Keeffe and O. M. Yaghi, *J. Am. Chem. Soc.*, 2009, **131**, 3875.

40 D. Britt, H. Furukawa, B. Wang, T. G. Glover and O. M. Yaghi, *Proc. Natl. Acad. Sci. U. S. A.*, 2009, **106**, 20637.
41 A. Goeppert, M. Czaun, R. B. May, G. K. S. Prakash, G. A. Olah and S. R. Narayanan, *J. Am. Chem. Soc.*, 2011, **133**, 20164–20167.
42 X. X. Wang, V. Schwartz, J. C. Clark, X. L. Ma, S. H. Overbury, X. C. Xu and C. S. Song, *J. Phys. Chem. C*, 2009, **113**, 7260–7268.
43 F. S. Su, C. Y. Lu, S. C. Kuo and W. T. Zeng, *Energy Fuels*, 2010, **24**, 1441–1448.

